

Multielement Analysis of Petroleum Products Using the Promising Technique of Optical Emission Spectrometry with Two-Jet Plasma

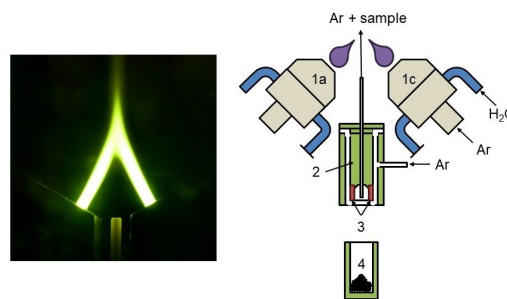
N. A. Orlov, A. V. Volzhenin, and N. S. Medvedev*

Nikolaev Institute of Inorganic Chemistry, Siberian Branch of Russian Academy of Sciences

Received: December 18, 2025; Revised: February 06, 2026; Accepted: February 08, 2026; Available online: February 08, 2026.

DOI: 10.46770/AS.2025.235

ABSTRACT: The main analytical challenges during multi-element analysis of petroleum product are related to the difficulties of sample introduction into the excitation and ionization sources and significant spectral matrix effects. The method of analysis of samples of the petroleum products by two-jet plasma optical emission spectrometry (TJP-OES) is proposed. The innovation lies primarily in application of TJP-OES for viscous organic samples (motor oil and heavy fuel oil), associated sample preparation strategy, optimized drying protocol and the demonstration of performance for a wide range of elements in challenging matrices. The proposed approach to sample preparation and measurement is dilution of the samples by organic solvent (kerosene) with subsequent drying on the graphite powder under IR lamp and TJP-OES analysis of mixture of graphite powder and the analyzed sample. This approach allows perform analysis of the petroleum products without the use of non-standard sample injection systems into atomization sources or labor-intensive sample preparation procedures. The limits of detection (LODs) of the analytes ranged from 10^{-6} to 10^{-3} % wt for 29 trace elements are achieved. Recovery values were from 70 to 130 % are obtained during «spike» experiment. Accuracy of proposed method was confirmed by comparison the results of analysis of the petroleum products by TJP-OES and optical emission spectrometry with inductively coupled plasma (ICP-OES). Thus, the applicability of the TJP-OES method for multi-element analysis of samples of the petroleum product is demonstrated.



Schematic diagram of TJP-OES: 1a/1c - electrodes (anode/cathode), 2 - spark discharge, 3 - electrode discharge, 4 - cup with sample.

INTRODUCTION

Crude oil is one of the most important resources of the 20th and 21st centuries.¹ For many years, it has been a primary source of energy. The main applications of crude oil are fuels and lubricants. Additionally, crude oil is a source of sulfur and its derivatives, certain metals (such as nickel, vanadium, rhenium, *etc.*), polar compounds, softeners, and more.

The origin and chemical composition of crude oil, its fractions and residues determine its physicochemical properties.² More than 60 trace elements have been found in oil, with half of them being metals.³ In natural oils and solid bitumens, metals are found in the

following forms: Cu, Fe, Pb, and U form true solutions; Zn, Cu, Ni, U, Ca, Mg, Fe, and V form colloidal solutions adsorbed on the active oil/water surface; Cu, Zn, Ge, and Au are found in polar resins as salts of organic acids; Hg, Sb, As, V, Ni, Fe, Cu, Co, Cr form organometallic compounds, and V and Ni form metalloporphyrin complexes. The development of oil fields containing elevated concentrations of metals, must be considered from the technological, environmental, and industrial-raw materials perspectives.⁴ For example, the presence of vanadium in oil leads to increased corrosion of casings, pipelines, tanks and refineries. Vanadium, which passes from oil into petroleum products, causes no less damage. When vanadium-containing fuels are burned in engines and boiler units, their service life is

significantly reduced. The environmental aspect is because many metals are highly toxic compounds and, entering the atmosphere, hydrosphere, and the earth's surface, have a negative impact on flora and fauna. It should be noted that vanadium is classified as a first-class environmentally hazardous product.⁵ The elemental composition of oil and petroleum products is usually determined using spectral methods such as atomic emission spectrometry (AAS) – ASTM 4628-16, optical emission spectrometry (OES) – ASTM 5185-13, and mass spectrometry (MS).^{6,7}

The metal concentrations provide valuable information about the age and origin of oil products (as indicated by the V/Ni ratio).⁸ The presence of metallic elements in fuel is undesirable even at low concentrations. Their determination is essential for assessing fuel quality and controlling air pollution.⁹ Moreover, the presence of metals complicates the refining process, and their presence in fuel can impair engine performance. Refined products are likely to exhibit higher toxicity than crude oil due to the modification of metals and the addition of new ones to the matrix. The relevance of using various additives in fuels and lubricants is growing. Additives help to increase the service life and efficiency of modern equipment, but they also contain various metal elements. For example, the introduction of anti-corrosion additives, consisting of various salts (such as salts of petroleum and sulfonic acids, calcium salts of nitrated oil, *etc.*) and acids (like alkenyl succinic and sulfonic acids), improves the protection of mechanical parts and oil from corrosion.¹⁰ In the case of additives, the quantitative determination of metals is necessary to monitor the physical and chemical properties of fuel and lubricants. Also, the relevance of analyzing waste products for the purpose of diagnosing and troubleshooting equipment and machines is growing.¹¹

In addition, the production of biofuels is becoming increasingly important, with biodiesel being the most common form. Biodiesel fuel must be blended with conventional petroleum diesel to produce a biodiesel blend, such as B5 (5% biodiesel with 95% petroleum diesel by volume).¹² Despite some physical differences between biofuels and fuels derived from oil, the approach to analysis is quite similar.¹³ And most of the techniques used for analyzing petroleum products can also be applied to biofuels.

The analysis of organic compounds presents a challenging task for OES methods due to the peculiarities of sample introduction into the excitation sources and significant non-spectral matrix effects. Non-spectral matrix effects are associated with the processes of aerosol formation and transfer, which cause changes in the amount of the analyte entering the plasma and makes the plasma less stable. Spectral matrix effects are mainly related to the formation of decomposition by-products (appearance of molecular bands in the spectrum) during atomization and ionization of the organic matrix “fragments.” In summary, the presence of organic compounds in the plasma leads to the deterioration of the limits of detections (LODs) of the analytes and

the accuracy of their content determination.

To reduce or eliminate matrix effects from complex organic substances, acid digestion or dilution with organic solvents is often employed. Dilution with organic solvents ensures rapid and simple sample preparation, but its disadvantages include the toxicity of the solvents, low stability of the analyte in the solution after dilution, and the need for calibration with solutions prepared using organic standards.^{14,15} Also dilution leads to a decrease in the analyte signal, an increase in the contribution of matrix effects and deterioration of the LODs of analytes. Dilution is most used in standard analytical methods. For example, in ASTM 5185-13, motor oils are analyzed using the ICP-OES method, 18 analytes (Ag, Al, B, Cd, Cr, Cu, Fe, Mg, Mo, Na, Ni, Pb, Sb, Si, Sn, Ti, W, Zn) can be determined, each of which can serve as a signal for wear in parts of the vehicle's powertrain. The ASTM 5185-13 method recommends using a standard USP oil, which does not contain analytes (for preparing comparison samples); it suggests using cadmium, cobalt, and/or yttrium as internal standards, and xylene or kerosene as solvents. It is mandatory to homogenize the analyzed samples using an ultrasonic bath or vortex mixer. The dilution factor for oils in this method is 10, which leads to a deterioration of LODs of the analytes by at least an order of magnitude.

In addition to dilution, various types of digestion are used for the analysis of petroleum and petroleum products, such as microwave-assisted autoclave digestion and acid digestion in open systems. Microwave digestion has several advantages over acid digestion: reduced acid consumption, minimized losses of volatile elements, and the ability to control higher temperatures. The ICP-OES method of oil analysis with microwave digestion is described. This method demonstrated LODs from 0.01 to 4.0 µg/g for 20 analytes: Al, Ba, Ca, Cd, Cr, Cu, Fe, K, Mg, Mn, Mo, Na, Ni, P, S, Sn, Sr, Ti, V, Zn. The disadvantage of microwave digestion is using of additional expensive equipment, which demands experience and high qualifications from personnel. Incomplete sealing of autoclaves, complex exothermic processes, “explosion” of autoclaves — all these factors may negatively affect the accuracy of sample preparation and the resulting analytical data. Acid digestion is a labor-intensive and time-consuming process that requires a large volume and variety of acids.¹⁶ The use of larger volumes of reagents increases the contribution of matrix effects and decreases LODs. It is important to clarify that such factors as 1) analyte loss during heating, 2) procedure duration, 3) contribution of matrix effects from the reagents used — these are general limitations inherent to both acid digestion in open systems and microwave digestion in autoclaves.

Extraction, similar to acid digestion, involves laborious sample preparation, with the added limitation of requiring the use of various toxic reagents. For the analysis of heavy petroleum residues, dilution and extraction methods were used;¹⁷ this

combination reduces preparation time compared to microwave digestion and achieves similar LODs, ranging from 0.03 to 5.4 $\mu\text{g/g}$ for 19 analytes (Ag, Al, Ba, Ca, Cd, Cr, Cu, Fe, Mg, Mn, Mo, Na, Ni, Pb, Si, Sn, Ti, V, Zn). In addition to the common sample preparation methods, the potential for analyzing dispersed systems is actively being explored. Among them, direct oil-in-water emulsions using surfactants (SAS),¹⁸ microemulsions¹⁹ and alternative systems for introducing samples into atomization sources are also used electrothermal vaporization²⁰ are particularly popular. Dispersed systems are actively being studied for analyzing objects of various natures for OES determination of a wide range of analytes.

Thus, to overcome the limitations discussed, it is necessary to develop a method for analyzing petroleum products with less labor-intensive sample preparation and less dilution of analyzed samples. Two-jet arc plasma optical emission spectrometry has several advantages that distinguish it from other excitation sources. For example, the TJP has higher power up to 15 kW, providing greater stability and less influence on the sample matrix composition compared to ICP. This allows achieving lower LODs compared to ICP-OES. The advantages of TJP include high efficiency of converting electrical energy into heat with a relatively simple instrumentation setup, ability to analyze solid samples of various natures and low gas consumption due to water cooling of the plasma torch heads. High power of TJP minimizes physical matrix effects, *i.e.*, non-spectral influences. The analytical capabilities of TJP-OES were studied during analysis of various objects: metals, alloys, ores, *etc.*^{21,22,23} The detection limits of Cr, Cu, Mn, Mo, Ni, Si, and V during the TJP-OES analysis of steel with spark ablation were determined in the range of 10^{-5} - 10^{-3} wt%. In present study the method for trace analysis of various petroleum products after evaporation of diluted samples on graphite powder under IR drying was developed. The innovation of present study lies primarily in application of TJP-OES for viscous organic samples (motor oil and heavy fuel oil), sample preparation strategy, optimized drying protocol and the demonstration of performance of TJP-OES for a wide range of elements in viscous organic samples.

EXPERIMENTAL

Reagents and materials. Nitric acid (10 M) was subjected to additional purification using a DuoPUR subboiler distillation unit (Milestone, Italy) before preparing analyzed samples. The possibility of using emulsions with the surfactant TX-100 (CAS 9002-93-1, not less than 99%, MP Biomedicals) was also explored. Aviation kerosene TS-1 (GOST 10227-86), is produced by direct distillation of middle distillate fractions of oil, used as a diluent. The behavior of various mixtures with petroleum products was determined throughout the study using high-purity graphite

powder. Multi-element standard reference solutions (MES) were used for experimental validation. The concentration of analytes in MES were next. MES-1: Al, Ca, Cd, Cr, Fe, K, Mg, Mn, Na, P, Zn 50 mg L⁻¹, Li 10 mg L⁻¹; MES-2: B, Bi, Co, Cu, Ga, In, Ni, Si, Ti, V 50 mg L⁻¹; MES-3: As, Pb, Rb, Sb, Se, Sn, Te 50 mg L⁻¹, Ba, Sr 20 mg L⁻¹, Ag, Au, Be 10 mg L⁻¹; Hg 5 mg L⁻¹; MES-4: Hf, Mo, Nb, Re, Ta, W, Zr 50 mg L⁻¹. Sample digestion system MS-10 (Himlab, Russia) was used for sample decomposition followed by ICP-OES analysis. Samples for repeatability control, control of interlaboratory reproducibility, error control and spike experiment were prepared using petroleum products diluted with kerosene and MES solutions according to the method described in section «Instrumentation, operating conditions and samples preparation». The heavy fuel oil (HFO) and motor oil were used as examples of petroleum products.

Instrumentation, operating conditions, and samples preparation.

The research was performed using a Fakel two-jet arc plasmatron and Grand spectrometer (VMK-Optoelectronica, Russia). Fakel consists of plasma heads, a power supply system, sample entry, gas management, and cooling (Fig. 1). The high-purity graphite powder sample is placed in an acrylic cup, which is positioned over a cylinder with an electrical spark ring discharge electrode on the lower end surface. When high-frequency voltage (~ 10 kV) is applied to the discharge electrode, radial breakdowns occur between the central and outer ring electrodes above the surface of the sample. The electrode materials are copper and tungsten. The shock waves generated by the discharge evenly agitate the powder surface. After sealing the "body-cup" unit with a locking nut, the transport gas flow enters the sample at the bottom

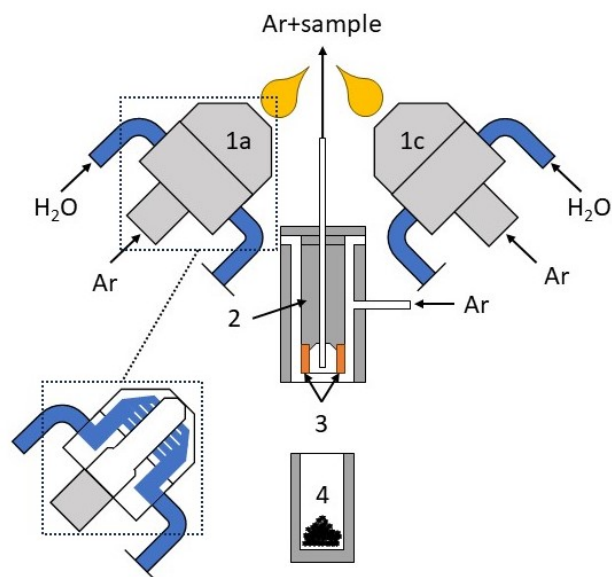


Fig. 1 Schematic diagram of TJP-OES: 1a/1c - electrodes (anode/cathode), 2 - spark discharge, 3 - electrode discharge, 4 - cup with sample.

bottom of the cup and, through a capillary tube in the center of the discharge electrode, carries the resulting aerosol into the excitation zone. The inner diameter of the supply tube is 1.5 mm. The arc current was 90 A, the angle between the plasma torch heads was 115–120 degrees, with the plasma jet merging angle ranging from 60 to 65 degrees. All transport components of the plasma torch were cleaned after each sample using compressed air and pure graphite powder. The spectrometer is designed according to the Paschen–Runge scheme and has a non-classical concave diffraction grating with two multichip assemblies (12 and 8 photodiode arrays forming a 0.5 cm radius). The working spectral ranges are from 190 to 350 and from 385 to 470 nm. For TJP-OES analysis oil samples were dried under a 500 W IR lamp at an irradiation distance of 10 cm.

The results of TJP-OES analysis of petroleum samples were carried out in conjunction with ICP-OES analysis using an ICPE-9800 (Shimadzu), with the instrumental parameters presented in Table S1. Sample preparation for ICP-OES analysis of petroleum products was as follows: a weighed portion of the petroleum product (0.1 g) was placed in a fluoroplastic autoclave and 10 ml of 10 M nitric acid was added, then preheated to 80 °C, after which it was placed in a microwave oven and heated to 230 °C. The temperature program is presented in Table S2.

RESULTS AND DISCUSSION

Optimization of sample preparation procedure. For TJP-OES analysis samples of petroleum products were dried on high-purity graphite powder. It is important to achieve a homogeneous mixture that does not clump together to ensure uniform supply into the two-jet arc plasma torch. The dryness of the samples was checked visually. Furthermore, the mixture should not stick to the spatula or form lumps during mixing.

Initially, attempts were made to dry petroleum products on graphite powder under an infrared (IR) lamp. Motor oil in volumes 50–100 μL was added to a 100 mg portion of graphite powder. The mixture was then placed in a sterile box under an IR lamp. However, after 24 hours, the resulting mixture remained a clumped mass of graphite powder and did not dry. Consequently, it was transferred to a tubular furnace and calcined at 200°C for several hours. Although using a tubular furnace helps dry oil samples on graphite powder, this method leads to contamination of the analyzed sample and loss of analytes due to calcination. Therefore, attempts were made to simplify the drying process. A few hours after the motor oil was added to the graphite powder, the mixture was acidified with concentrated nitric acid. However, this approach also failed to produce a homogeneous, dry, non-viscous mixture, requiring further drying in a tubular furnace at 200°C. So, the motor oil could not be dried on graphite powder

without dilution. A similar approach was used with TX-100. 5 mL of an aqueous solution of TX-100 (with a surfactant concentration of 0.02 mol/L) was added to 2 ml of motor oil. This mixture also did not allow obtaining a homogeneous dry mixture of graphite powder and petroleum product. Therefore, a decision was made to use an organic solvent — aviation kerosene. First, the motor oil was placed in a test tube and weighed. Then kerosene was added, and the sample was reweighed to ensure the dilution factor did not exceed 10 times by mass. The resulting mixture was then applied in a volume of 100 μL to 100 mg of graphite powder, placed under an IR lamp, and dried for 3 h. This method proved effective, as it allowed the motor oil and kerosene mixture to dry on graphite powder, yielding a homogeneous, non-clumping mixture of graphite powder and the analyzed sample. Although a 10-fold dilution with kerosene proved suitable for drying the sample analyzed, it was necessary to determine whether a lower dilution factor could be used. For this, motor oil was diluted with kerosene at ratios ranging from 4 to 10 times and applied to graphite powder. It was found that a 6.5-fold dilution with kerosene was optimal, as it allowed the mixture to dry to a homogeneous state within 10 h under an IR lamp. A similar procedure was performed for HFO provided by the template synthesis group at the Boreskov Institute of Catalysis, Siberian Branch of the Russian Academy of Sciences. As a result, it was established that the optimal sample preparation method involved dilution in kerosene at a 6.5-fold ratio, followed by application to graphite powder.

Calculation of detection limits of analytes. Spectral lines with the highest I/S ratio (I - analyte signal intensity, S - background signal intensity) and minimal matrix influences were used as analytical lines (Fig. 2). The LODs were calculated by the 3s criterion. For this, a residual petroleum products sample with the lowest impurity content was analyzed 10 times under the selected analysis conditions. Calibration was built on solid and aqueous samples of comparisons mixed with graphite powder. The LODs

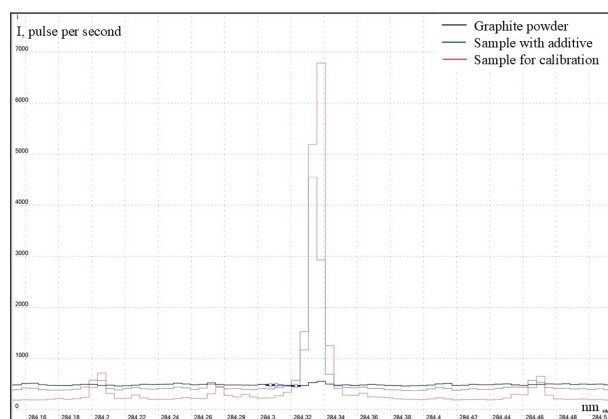


Fig. 2 Chromium 284.3249 nm.

Table 1. Comparison of the LODs provided by TJP-OES analysis and ASTM 5185-13 method

| Analyte | TJP-OES LODs, of analyte % wt | ASTM 5185- 13, % wt | Analyte | TJP-OES LODs, of analyte % wt | ASTM 5185- 13, % wt |
|-----------|--|------------------------------|---------|--|------------------------------|
| Ag | 2×10 ⁻⁵ | 5×10 ⁻⁵ | Mo | 5×10 ⁻⁴ | 5×10 ⁻⁴ |
| Al | 4×10 ⁻⁵ | 6×10 ⁻⁴ | Na | 5×10 ⁻⁴ | 7×10 ⁻⁴ |
| B | 3×10 ⁻⁵ | 4×10 ⁻⁴ | Nb | 5×10 ⁻⁴ | - |
| Ba | 2×10 ⁻⁴ | 5×10 ⁻⁵ | Ni | 2×10 ⁻⁴ | 5×10 ⁻⁴ |
| Be | 7×10 ⁻⁷ | - ^a | P | 5×10 ⁻⁴ | 1×10 ⁻³ |
| Bi | 9×10 ⁻⁵ | - | Pb | 5×10 ⁻⁴ | 1×10 ⁻³ |
| Ca | 7×10 ⁻⁴ | 4×10 ⁻³ | S | - | 9×10 ⁻² |
| Cd | 2×10 ⁻⁶ | - | Sb | 2×10 ⁻³ | - |
| Co | 2×10 ⁻⁴ | - | Si | 1×10 ⁻⁴ | 8×10 ⁻⁴ |
| Cr | 2×10 ⁻⁴ | 1×10 ⁻⁴ | Sn | 2×10 ⁻⁴ | 1×10 ⁻³ |
| Cu | 2×10 ⁻⁴ | 2×10 ⁻⁴ | Ti | 7×10 ⁻⁵ | 5×10 ⁻⁴ |
| Fe | 2×10 ⁻⁴ | 2×10 ⁻⁴ | V | 1×10 ⁻³ | 1×10 ⁻⁴ |
| K | 1×10 ⁻³ | 4×10 ⁻³ | W | 1×10 ⁻³ | - |
| Mg | 8×10 ⁻⁵ | 5×10 ⁻⁴ | Zn | 3×10 ⁻⁵ | 6×10 ⁻³ |
| Mn | 5×10 ⁻⁵ | 5×10 ⁻⁴ | | | |

^aNot given by ASTM 5185-13 method.

obtained for TJP-OES analysis of petroleum products in the range from 10⁻⁶ to 10⁻³ % weight for 29 trace elements. For most analytes, the LODs were decreased by an order or more compared to the standard method of analyzing motor and used motor oils by ASTM 5185-13 (Table 1). LODs were reduced through more efficient atomization and excitation of elements and dilution factor. The spike experiment was performed to confirm the accuracy of the proposed method of TJP-OES analysis (Tables S3 and S4). The spike concentrations were chosen relative to the method's LODs. First, petroleum product samples of known composition were dried on graphite powder. Then, a known amount of trace elements was added to the same quartz cup. After drying, TJP-OES analysis was performed. Trace elements were added at a level of 1×10⁻⁴, 5×10⁻⁴ and 1×10⁻³ % wt. This sample was analyzed at different times by the same operator in the same laboratory. The experiment was carried out 10 times for HFO and 5 times for motor oil. The standard deviation for the elements presented in the sample, the mathematical expectation of the systematic error and the error of the analysis were calculated. Factors that can influence higher or lower recovery rates are primarily related to impurities in the HFO and motor oil itself. Calcium, potassium, sodium, nickel, and vanadium (approximately 0.001% by weight) are present in the HFO sample itself in high quantities for the spike experiment. Motor oil contains approximately 0.01% by weight of boron, and because of this, a positive bias in the boron concentrations may be observed in parallel experiments with HFO and motor oil. Plasma torch heads are made of copper, which in turn also leads to a slight positive bias in the measured concentrations. Despite all the above, recovery from 70 to 130 % was found for the studied analytes. Thus, the proposed method of TJP-OES analysis petroleum products allows us to obtain reliable quantitative results. Note that this experiment is time-consuming and several samples must be prepared at different

concentration levels. Trace elements must be coated on graphite powder and allowed to dry. Furthermore, it is impossible to prepare a single solution of all the required elements from which to sample, due to the diverse chemical properties of multi-element solutions.

Crude oil is a complex mixture of hydrocarbons that can be separated into fractions according to boiling point by atmospheric and vacuum distillation. Typical fractions include refinery gases (C₁-C₄, <30 °C), naphtha (30-180 °C), gasoline (40-200 °C), kerosene (180-260 °C), diesel/light gas oil (250-350 °C), lubricating oil fractions (>350 °C), and the heaviest residuals such as HFO, bitumen, or asphalt (>500 °C).^{24,25} HFO, obtained near the very end of the distillation process, is among the most viscous petroleum products, with a viscosity comparable to that of machine oils. To develop a robust multi-element analytical method for petroleum products, we focused on HFO as the most challenging matrix. Kinetic viscosity measurements of the HFO samples provided by the Template Synthesis Laboratory of the Institute of Catalysis SB RAS showed that they were six times or more viscous than typical machine oils. Full multi-element analysis was performed using TJP-OES, which allowed determination of 29 trace elements with limits of detection ranging from n·10⁻⁶ to n·10⁻³ % by weight. Moreover, during the study of sample preparation, it was established that the kerosene fraction and below do not require additional dilution with organic solvents. Based on these results, we conclude that the developed TJP-OES method is suitable for the most viscous petroleum fractions and, by extension, readily applicable to lighter, less viscous petroleum products, for which sample dilution with kerosene may be reduced or even omitted, resulting in lower LODs.

Using repeatability values from ASTM 5185-13, Shewhart charts were constructed from the obtained analysis results for the sample with introduced trace elements. Then using the repeatability and reproducibility equations from ASTM 5185-13, for each element separately:

$$\sigma_{r(R)} = aCb; (a, b = \text{const}, C - \text{concentration}) \quad (1)$$

With the substituted known certified value, the following were constructed: the center line – CL, the warning control limit – WCL, and the action control limit – ACL:

- Repeatability control: in the case of two control determinations: the control result is the value $r_k = x_{max} - x_{min}$, the average line is determined by the value $go\ CL - r_0 = 1.128\sigma_r$, $WCL - r_2 = 2.834\sigma_r$; $ACL - r_3 = 3.686\sigma_r$.
- Control of interlaboratory reproducibility: in the case of two control determinations: the control result is the value $R_k = |\underline{x}_1 - \underline{x}_2|$, where $\underline{x}_{1(2)}$ is the result of the primary (repeat)

control measurement; the $CL - R_0 = 1.128\sigma_R$, $WCL - R_2 = 2.834\sigma_R$; $ACL - R_3 = 3.686\sigma_R$.

- Error control. Result of control is the value of $K_k = \bar{x} - C$, where \bar{x} is the result of the control measurement, C – is the certified value of the determined indicator in the control sample; the CL is determined by the value of $K_0 = 0$, the WCLs are equal to $K_{2,B} = K_2 = 2\sigma(\Delta_L)$, where $\pm\Delta_L$ is the characteristic of the error of the analysis results ($\Delta_L=20\%$ for TJP-OES); the ACLs are equal $K_{3,B} = -K_3 = 3\sigma(1.5\Delta_L) = 1.5K_2$.

When interpreting repeatability and intra-laboratory precision control charts, the following events may serve as a signal of a

possible violation of the stability of the analytical process:

- 1) one point is out of range;
- 2) nine points in a row are above the midline;
- 3) six ascending dots in a row check;
- 4) fourteen alternately increasing and decreasing dots;
- 5) two of three consecutive points are above the warning limit;
- 6) four out of five consecutive points are above half the warning zone boundary.

Shewhart charts for the presented elements, most of the values fall in the area between the CL and the WCL, which indicates the relevance of the data we received (Fig. 3).

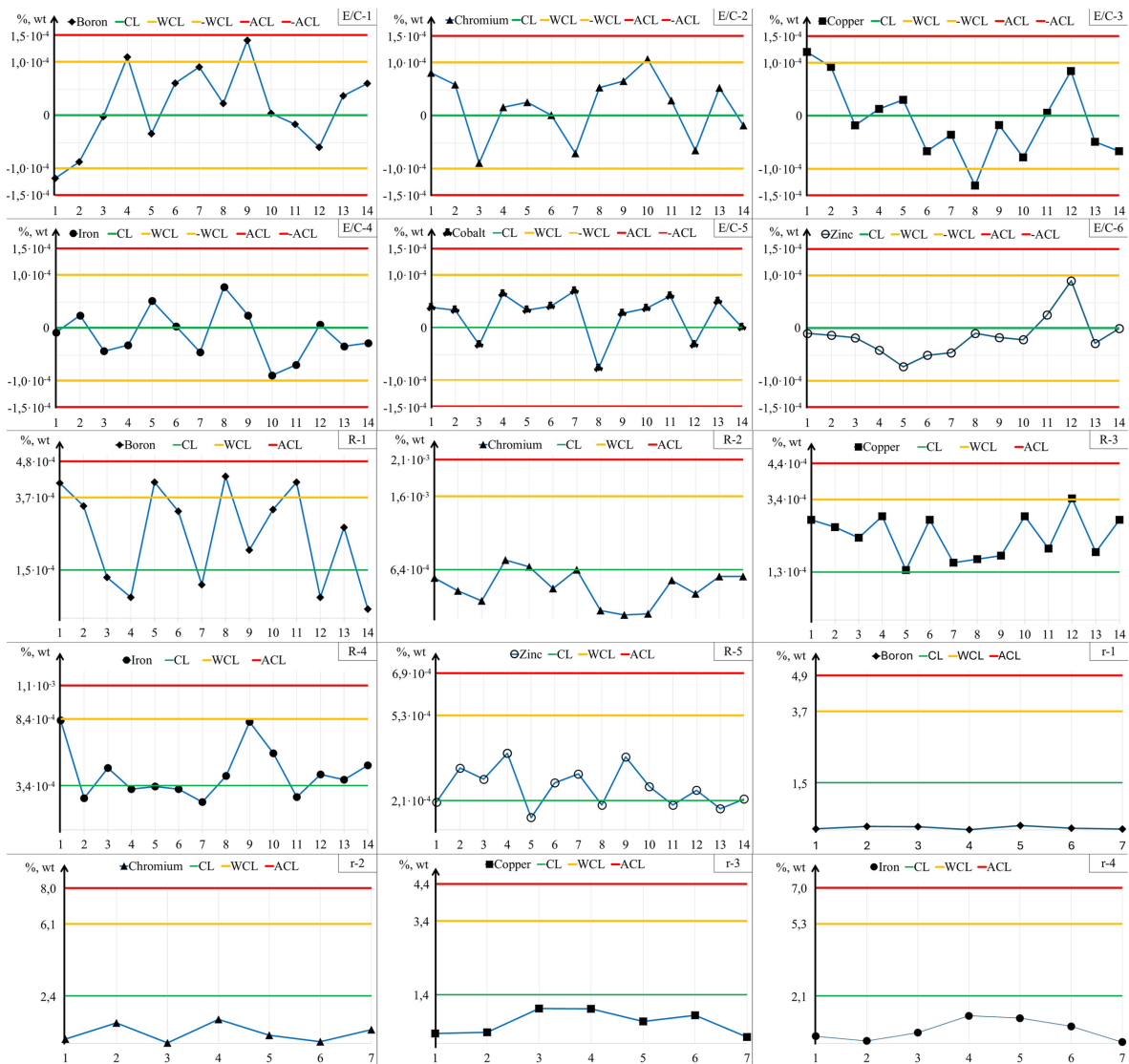


Fig. 3 Repeatability (R-i, i=1-5), interlaboratory reproducibility (r-j, j=1-4), and error control of analytes (E/C-1, l=1-6). Center line – CL, the warning control limit – WCL, and the action control limit – ACL.

Table 2. Results of TJP-OES and ICP-OES analysis of motor oil and heavy fuel oil (n=5, P=0.95). Results of analysis show the values $\bar{X} \pm \Delta$, where $\Delta = \frac{s \cdot t}{\sqrt{n}}$. The critical value of the Fisher test ($f_1, f_2 = 4; n_1, n_2 = 5$) = 6.39. The critical value of the t-criteria ($f = n_1 + n_2 - 2 = 8, p = 0.95$) = 2.31.

| Analyte | Motor oil 5W-30 ($v=0.1 \text{ cm}^2/\text{sec}$) | | | | | | HFO №1 ($v=14.7 \text{ cm}^2/\text{sec}$) | | | | | |
|---------|---|--------|--------------------------------|--------|---------------------------|------------------|---|--------|--------------------------------|--------|---------------------------|------------------|
| | ICP-OES | RSD, % | TJP-OES | RSD, % | $F(S_1^2/S_2^2, S_1>S_2)$ | t_{exp} | ICP-OES | RSD, % | TJP-OES | RSD, % | $F(S_1^2/S_2^2, S_1>S_2)$ | t_{exp} |
| Al | $(1.1 \pm 0.3) \times 10^{-3}$ | 24 | $(1.2 \pm 0.2) \times 10^{-3}$ | 15 | 2.3 | 0.28 | $(1.2 \pm 0.2) \times 10^{-3}$ | 15 | $(1.3 \pm 0.2) \times 10^{-3}$ | 13 | 1.0 | 0.35 |
| B | $(2.1 \pm 0.5) \times 10^{-2}$ | 21 | $(1.5 \pm 0.4) \times 10^{-2}$ | 23 | 1.6 | 0.94 | $(2.2 \pm 0.5) \times 10^{-4}$ | 20 | $(2.6 \pm 0.6) \times 10^{-4}$ | 20 | 0.7 | 0.51 |
| Ba | $(3.6 \pm 0.3) \times 10^{-5}$ | 22 | $<(2 \times 10^{-4})$ | - | - | - | $(1.2 \pm 0.3) \times 10^{-4}$ | - | $<(2 \times 10^{-4})$ | - | - | - |
| Be | $<(1 \times 10^{-5})$ | - | $<(7 \times 10^{-7})$ | - | - | - | $<(1 \times 10^{-5})$ | - | $<(7 \times 10^{-7})$ | - | - | - |
| Bi | $<(1 \times 10^{-5})$ | - | $<(5 \times 10^{-5})$ | - | - | - | $<(1 \times 10^{-5})$ | - | $<(5 \times 10^{-5})$ | - | - | - |
| Ca | 0.19 ± 0.05 | 23 | 0.15 ± 0.03 | 17 | 2.8 | 0.69 | $(5.2 \pm 0.9) \times 10^{-3}$ | 15 | $(6.4 \pm 1.1) \times 10^{-3}$ | 15 | 0.7 | 0.84 |
| Cd | $<(5 \times 10^{-6})$ | - | $<(2 \times 10^{-6})$ | - | - | - | $<(5 \times 10^{-6})$ | - | $<(2 \times 10^{-6})$ | - | - | - |
| Co | $<(1 \times 10^{-5})$ | - | $<(2 \times 10^{-4})$ | - | - | - | $<(1 \times 10^{-5})$ | - | $<(2 \times 10^{-4})$ | - | - | - |
| Cr | $(2.2 \pm 0.4) \times 10^{-4}$ | 16 | $(2.9 \pm 0.5) \times 10^{-4}$ | 15 | 0.6 | 1.09 | $(5.0 \pm 0.9) \times 10^{-4}$ | 16 | $(5.1 \pm 1.0) \times 10^{-4}$ | 17 | 0.8 | 0.07 |
| Cu | $<(9 \times 10^{-5})$ | - | $<(5 \times 10^{-4})$ | - | - | - | $<(1 \times 10^{-4})$ | - | $<(5 \times 10^{-4})$ | - | - | - |
| Fe | $(8.7 \pm 1.9) \times 10^{-4}$ | 19 | $(9.6 \pm 1.1) \times 10^{-4}$ | 10 | 3.0 | 0.41 | $(3.4 \pm 0.5) \times 10^{-3}$ | 13 | $(4.0 \pm 0.8) \times 10^{-3}$ | 17 | 0.4 | 0.64 |
| K | $<(9 \times 10^{-4})$ | - | $<(1 \times 10^{-3})$ | - | - | - | $<(9 \times 10^{-4})$ | - | $<(1 \times 10^{-3})$ | - | - | - |
| Mg | $(9.8 \pm 2.1) \times 10^{-4}$ | 19 | $(8.9 \pm 1.7) \times 10^{-4}$ | 17 | 1.5 | 0.33 | $(1.7 \pm 0.2) \times 10^{-4}$ | 10 | $(1.5 \pm 0.2) \times 10^{-4}$ | 12 | 1.0 | 0.71 |
| Mn | $<(5 \times 10^{-5})$ | - | $<(5 \times 10^{-5})$ | - | - | - | $(2.8 \pm 0.5) \times 10^{-4}$ | 16 | $(3.3 \pm 0.2) \times 10^{-4}$ | 5 | 6.3 | 0.93 |
| Mo | $(7.3 \pm 1.1) \times 10^{-3}$ | 13 | $(5.1 \pm 0.9) \times 10^{-3}$ | 15 | 1.5 | 1.55 | $<(6 \times 10^{-5})$ | - | $<(5 \times 10^{-4})$ | - | - | - |
| Na | $(2.1 \pm 0.5) \times 10^{-3}$ | 21 | $(2.6 \pm 0.7) \times 10^{-3}$ | 23 | 0.5 | 0.58 | $(2.1 \pm 0.6) \times 10^{-3}$ | 21 | $(1.7 \pm 0.2) \times 10^{-3}$ | 10 | 6.3 | 0.74 |
| Ni | $<(7 \times 10^{-5})$ | - | $<(2 \times 10^{-4})$ | - | - | - | $(8.8 \pm 1.2) \times 10^{-4}$ | 12 | $(9.7 \pm 2.9) \times 10^{-4}$ | 26 | 0.2 | 0.29 |
| P | 0.068 ± 0.020 | 26 | 0.081 ± 0.023 | 25 | 0.8 | 0.43 | $<(5 \times 10^{-4})$ | - | $<(5 \times 10^{-4})$ | - | - | - |
| Pb | $<(1 \times 10^{-4})$ | - | $<(5 \times 10^{-4})$ | - | - | - | $<(1 \times 10^{-4})$ | - | $<(5 \times 10^{-4})$ | - | - | - |
| Sb | $<(1 \times 10^{-4})$ | - | $<(1 \times 10^{-3})$ | - | - | - | $<(1 \times 10^{-4})$ | - | $<(1 \times 10^{-3})$ | - | - | - |
| Si | $(5.6 \pm 1.0) \times 10^{-3}$ | 16 | $(4.9 \pm 0.9) \times 10^{-3}$ | 16 | 1.2 | 0.52 | $(1.4 \pm 0.3) \times 10^{-2}$ | 19 | $(1.5 \pm 0.2) \times 10^{-2}$ | 12 | 2.3 | 0.28 |
| Ti | $<(3 \times 10^{-5})$ | - | $<(7 \times 10^{-5})$ | - | - | - | $(3.4 \pm 0.6) \times 10^{-4}$ | 15 | $(4.4 \pm 0.8) \times 10^{-4}$ | 16 | 0.6 | 1.00 |
| V | $<(1 \times 10^{-4})$ | - | $<(1 \times 10^{-3})$ | - | - | - | $(2.0 \pm 0.4) \times 10^{-2}$ | 17 | $(2.3 \pm 0.5) \times 10^{-2}$ | 19 | 0.6 | 0.47 |
| W | $<(2 \times 10^{-4})$ | - | $<(1 \times 10^{-3})$ | - | - | - | $<(2 \times 10^{-4})$ | - | $<(1 \times 10^{-3})$ | - | - | - |
| Zn | $(7.7 \pm 1.0) \times 10^{-2}$ | 11 | $(7.2 \pm 1.3) \times 10^{-2}$ | 16 | 0.6 | 0.30 | $(1.2 \pm 0.2) \times 10^{-4}$ | 15 | $(1.1 \pm 0.2) \times 10^{-4}$ | 16 | 1.0 | 0.35 |

Petroleum products analysis. The accuracy of the TJP-OES method was also tested by comparing the results of TJP-OES and ICP-OES analysis of several petroleum products samples such as motor oil and HFO of different fractions. The analysis of petroleum product samples was carried out using the developed method of TJP-OES analysis and ICP-OES analysis. The ICP-OES method was used to evaluate accuracy of the method of TJP-OES analysis, Table 2 and Table S5 shows results of TJP-OES and ICP-OES analysis of motor oil, used oil and two HFO samples. Obtained values were compared by the Fisher test and t-criteria. The critical value of the Fisher test ($f_1, f_2=4; n_1, n_2 = 5$) = 6.39 and the critical value of the t-criteria ($f = n_1+n_2-2= 8, P = 0.95$) = 2.31. Experimental values of Fisher test range from 0.01 to 6.3 and experimental values of t-criteria range from 0 to 2.24. These values do not exceed the theoretically permissible values which confirms the consistency of the results obtained by the two methods.

CONCLUSION

A TJP-OES method for analyzing various petroleum products was developed. This method can be used to analyze products from both the light and heavy fractions of crude oil. Using a combination of IR and drying on the graphite powder provided universal sample preparation for different petroleum products. The TJP-OES

method provides the possibility of analysis without the use of non-standard sample injection systems into atomization sources or labor-intensive sample preparation procedures. The LODs of the analytes ranged from 10^{-6} to 10^{-3} % weight for 29 trace elements. The statistical processing of the data was performed, with the construction of Shewhart maps. Results of the spike experiment for the TJP-OES method were obtained, as well as good agreement between the ICP-OES and TJP-OES analyses of petroleum product samples.

AUTHOR INFORMATION



Nickolay Sergeevich Medvedev received his specialist degree in 2011 from the Novosibirsk State University and PhD in 2015 from the Nikolaev Institute of Inorganic Chemistry, Siberian Branch of Russian Academy of Sciences (NIIC SB RAS). He is a head of the Analytical laboratory of the NIIC SB RAS. His major

research interests are mass-spectrometry, optical emission spectrometry, preliminary concentration of trace elements, laser ablation and electrothermal vaporization and their applications to the analysis of high-purity substances and functional materials. He is author or co-author of over 40 articles published in peer-reviewed scientific journals, with an h-index

of 9 (Scopus).

Corresponding Author

* N. S. Medvedev

Email address: medvedev@niic.nsc.ru

Notes

The authors declare no competing financial interest.

ACKNOWLEDGMENTS

This study was funded by the Ministry of Science and Higher Education of the Russian Federation, project number 125021302133-1. We gratefully acknowledge the Template Synthesis Laboratory of the Boreskov Institute of Catalysis SB RAS for providing the HFO samples.

REFERENCES

1. O. F. Glagoleva and V. M. Kapustin, *Pet. Chem.*, 2018, **58**, 1–7. <https://doi.org/10.1134/S0965544118010097>
2. L. Poirier, J. Nelson, and D. Leong, *Energ. Fuel.*, 2016, **30**, 3783–3790. <https://doi.org/10.1021/acs.energyfuels.5b02997>
3. G. S. Simonyan, Scientific Review. Technical Sciences, 2016, **4**, 77–100. <http://www.id-yug.com/images/id-yug/Bulatov/2019/5/PDF/2019-5-120-123.pdf>
4. M. Yu. Nesterenko, A. V. Tsviak, G. A. Ponomareva, and O. A. Kapustina, *Atlantis Highlights in Materials Science and Technology*, 2019, **1**, 370–374. <https://doi.org/10.2991/isees-19.2019.72>
5. F. A. C. Amorim, B. Welz, A. C. S. Costa, F. G. Lepri, M. G. R. Vale, and S. L. C. Ferreira, *Talanta*, 2007, **72**, 349–359. <https://doi.org/10.1016/j.talanta.2006.12.015>
6. R. Sanchez, J.L. Todoli, Ch.-Ph. Lienemann, and J.-M. Mermet, *Spectrochim. Acta B*, 2013, **88**, 104–126. <https://doi.org/10.1016/j.sab.2013.06.005>
7. X. Xiang, W. Jiao, L. Cheng, and Y. Zhao, *Adv. Mater. Res.*, 2014, **834–836**, 340–344. <https://doi.org/10.4028/www.scientific.net/AMR.834-836.340>
8. E. Yu. Savonina, O. N. Katasonova, and T. A. Maryutina, *Inorg. Mater.*, 2022, **58**, 1479–1483. <https://doi.org/10.1134/S0020168522140126>
9. M. das G. A. Korn, D. S. S. dos Santos, B. Welz, M. G. R. Vale, A. P. Teixeira, D. de C. Lima, and S. L. C. Ferreira, *Talanta*, 2007, **73**, 1–11. <https://doi.org/10.1016/j.talanta.2007.03.036>
10. K.M. Shwetha, B. M. Praveen, and B. K. Devendra, *Results in Surfaces and Interfaces*, 2024, **16**, 100258. <https://doi.org/10.1016/j.rsufi.2024.100258>
11. R. Grimmig, S. Lindner, P. Gillemot, M. Winkler, and S. Witzleben, *Talanta*, 2021, **232**, 122431. <https://doi.org/10.1016/j.talanta.2021.122431>
12. R. Grimmig, S. Lindner, P. Gillemot, M. Winkler, and S. Witzleben, *Talanta*, 2021, **232**, 122431. <https://doi.org/10.1016/j.talanta.2021.122431>
13. Z. Yang, K. Shah, C. Pilon-McCullough, R. Faragher, P. Azmi, B. Hollebone, B. Fieldhouse, C. Yang, D. Dey, P. Lambert, and V. Beaulac, *Renew. Energy*, 2024, **224**, 120151. <https://doi.org/10.1016/j.renene.2024.120151>
14. R. Q. Aucélio, R. M. de Souza, R. C. de Campos, N. Miekeley and C. L. P. da Silveira, *Spectrochim. Acta B*, 2007, **62**, 952–961. <https://doi.org/10.1016/j.sab.2007.05.003>
15. O. N. Grebneva-Balyuk, I. V. Kubrakova, and O. A. Tyutyunnik, *J. Anal. Chem.*, 2021, **76**, 218–226. <https://doi.org/10.31857/S004445022103004X>
16. M. Turunen, S. Peräniemi, M. Ahlgren, and H. Westerholm, *Anal. Chim. Acta*, 1995, **311**, 85–91. [https://doi.org/10.1016/0003-2670\(95\)00166-W](https://doi.org/10.1016/0003-2670(95)00166-W)
17. T. A. Maryutina and N. S. Musina, *J. Anal. Chem.*, 2012, **67**, 959–967. <https://doi.org/10.1134/S106193481210005X>
18. M. G. R. Vale, I. C. F. Damin, A. Klassen, M. M. Silva, B. Welz, A. F. Silva, F. G. Lepri, D. L. G. Borges, and U. Heitmann, *Microchem. J.*, 2004, **77**, 131–140. <https://doi.org/10.1016/j.microc.2004.02.007>
19. R. M. de Souza, A. L. S. Meliande, C. L. P. da Silveira, and R. Q. Aucélio, *Microchem. J.*, 2006, **82**, 137–141. <https://doi.org/10.1016/j.microc.2006.01.005>
20. Z. Hou, Z. Wang, J. Liu, W. Ni, and Z. Li, *Opt. Express*, 2013, **21**, 15974–15979. <https://doi.org/10.1364/oe.21.015974>
21. A. V. Kuptsov, A. V. Volzhenin, V. A. Labusov, and A. I. Saprykin, *J. Anal. At. Spectrom.*, 2020, **35**, 2600–2608. <https://doi.org/10.1039/D0JA00313A>
22. A. V. Kuptsov, A. V. Volzhenin, V. A. Labusov, and A. I. Saprykin, *Spectrochim. Acta B*, 2021, **177**, 106047. <https://doi.org/10.1016/j.sab.2020.106047>
23. A. V. Kuptsov, N. S. Medvedev, O. V. Lundovskaya, A. I. Saprykin, and V. A. Labusov, *J. Anal. At. Spectrom.*, 2021, **36**, 2669–2677. <https://doi.org/10.1039/D1JA00286D>
24. J. G. Speight, *Handbook of Petroleum Refining*, CRC Press: Boca Raton, FL, 2016. <https://doi.org/10.1201/9781315374079>
25. D. S. J. Jones and P. R. Pujadó, *Handbook of Petroleum Processing*, Springer: Dordrecht, 2006. <https://www.vitalsource.com/products/handbook-of-petroleum-processing-v9781402028205>